Two-Photon Optical Beam-Induced Current Microscopy of Light-Emitting Diodes

Godofredo S. Bautista Jr.*, Carlo Mar Y. Blanca, and Caesar A. Saloma
National Institute of Physics, University of the Philippines,
Diliman, Quezon City 1101
E-mail: gbautista@nip.upd.edu.ph

ABSTRACT

We demonstrate two-photon optical beam-induced current (2P-OBIC) microscopy of light-emitting diodes (LEDs). We utilized a Ti:Sapphire femtosecond laser source operating at 800 nm to derive the 2P-OBIC signal from a 605 nm band-gap LED. The spatial confinement of free carrier generation only at the focus and the quadratic dependence of the 2P-OBIC signal on excitation power are the key principles in two-photon excitation. As a consequence, superior image quality evident in the 2P-OBIC images of LEDs are obtained. These features decrease the linear absorption and wide-angle scattering effects plaguing single-photon optical beam-induced current (1P-OBIC) technique, thereby increasing the resolution of the imaging system in the axial and lateral directions. Thus, the attainment of good axial discrimination in the LED samples is obtained even without a confocal pinhole. In addition, 2P-OBIC images reveal local variations in free carrier densities which are not evident in the single-photon excitation.

INTRODUCTION

When a laser beam with energy higher than the band-gap energy of the *p-n* junction irradiates semiconductors, generation of electron-hole pairs occurs and flow in the semiconductor to produce electrical current (Takasu, 2001). Measuring this current and mapping them on a display result to an optical beam-induced current (OBIC) image. This has become a major tool in the detection of defects in semiconductor devices (Wilson & Sheppard, 1984). However, a disadvantage of this technique is its inability to discriminate the localizations of the current distribution in the semiconductor since it is insensitive to focal positions (Koyama et al., 1999). Recently, researchers have devised a method to impart axial resolution to OBIC images from information derived from corresponding confocal reflectance images (Daria et al., 2002; Miranda & Saloma, 2003; Cemine et al., 2004).

We approach this problem by introducing nonlinearity in the photon absorption process to generate free carriers which can be externally detected as current flow. OBIC via two-photon excitation (2P-OBIC) has been developed to visualize free carrier densities in the semiconductor (Xu & Denk, 1997). In 2P-OBIC, each electron-hole pair is generated via absorption of the energies of two photons. It takes advantage of the quadratic dependence of the generated photocurrent on the excitation power and the confined illumination only at the focus as shown in two-photon fluorescence imaging (Denk et al., 1990). 2P-OBIC microscopy has also been utilized in backside imaging of flip chips, integrated circuits, and indium gallium nitride light-emitting diodes (Xu & Denk, 1999; Kao et al., 1999; Ramsay & Reid, 2002).

---

*Corresponding author

Here, we construct a two-photon optical beam-induced current microscope to image and characterize light-emitting diodes using a femtosecond laser source and a stage-scanning microscope. We compare free carrier generation, axial resolution, and image formation of 2P-OBIC with 1P-OBIC using a 543 nm HeNe laser. Results unraveled the characteristics of these semiconductor devices previously unseen by the 1P-OBIC technique.

EXPERIMENT

The schematic diagram of the stage-scanning custom-built microscope used in investigating 2P-OBIC is shown in Fig. 1. The illumination source used is a mode-locked Ti:Sapphire femtosecond pulse laser at 800 nm (Tsunami, Spectra-Physics) pumped by a frequency-doubled solid-state laser (Millennia, Spectra-Physics). A neutral density filter (NDF) is used to attenuate the excitation source. The beam is reflected by a relay of mirrors (M1 and M2) and later expanded by a two-lens telescope composed of L1 ($f = 25$ mm) and L2 ($f = 200$ mm). The resulting collimated beam is then directed to an infinity-corrected objective lens (OBJ, Olympus UPLAN Fl, 20x, 0.5 NA) overfilling its back aperture.

The objective focuses the excitation beam on the light-emitting diode (LED) sample mounted on the three-axis (x,y,z) motorized stage (Thorlabs, PT3-Z6) driven by a motion-controller card (Thorlabs, DCX-PCI100). Codes for stage scanning and image acquisition are all written in LabVIEW. The OBIC signals as a function
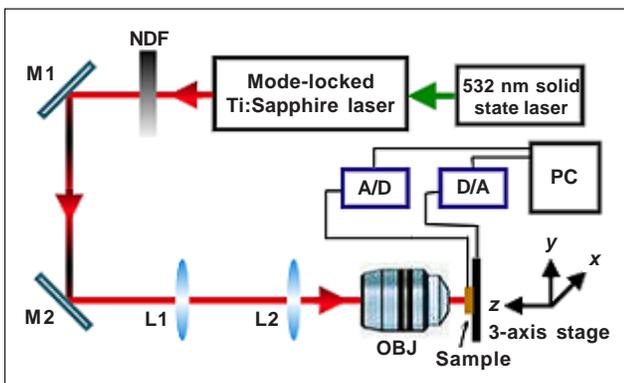
of sample position are utilized to build the corresponding image of the sample at the focal plane. Analog-to-digital (A/D) and digital-to-analog (D/A) conversion is accomplished with a 12-bit data-acquisition board (National Instruments, 6024E).

The LED samples are commercially available and exhibit electroluminescence with a peak at 605 nm. Throughout the scans, the average power which is measured before the objective lens is varied from 0.5 to 2.5 mW.

In order to generate 1P-OBIC, we replaced the femtosecond laser with an 8 mW HeNe laser operating at 543 nm. The imaging optics and acquisition system were not changed.

RESULTS

Shown in Fig. 2 is the incident power dependence of the OBIC signals for the LED sample. The quadratic dependence of the OBIC signal on the excitation power is expected for 2P-OBIC and the linear dependence for 1P-OBIC. We experimentally verified this for the 2P-OBIC process where the exponent of the excitation power is 1.9962. On the other hand, 1P-OBIC exhibited a linear behavior with a corresponding slope of 0.9095.

Because of the nonlinear behavior of 2P-OBIC, only regions near the focal volume generate current. This

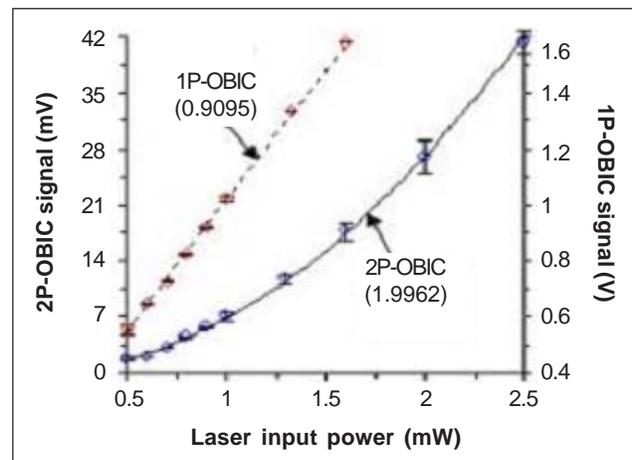Fig. 1. Schematic diagram of the stage-scanning 2P-OBIC microscope used.

Fig. 2. Power dependence of the generated OBIC signal. The slopes of the 2P-OBIC and 1P-OBIC responses are 1.9962 and 0.9095, respectively.
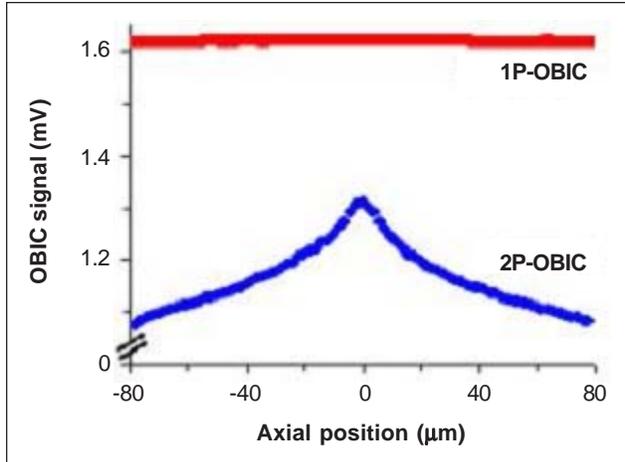
Fig. 3. Focal dependence of the generated OBIC signal. Throughout the scanned axial positions, 2P-OBIC changes while 1P-OBIC remains insensitive. The 2P-OBIC axial profile has a FWHM value of 50 μm.

Fig. 4. 2P-OBIC imaging of LED with and without mode-locked illuminations. Image size is 625 x 625 μm.

characteristic is clearly seen in Fig. 3 where the photocurrent signal is plotted against the axial position obtained by moving the sample along the z axis. The largest measured 2P-OBIC signal is found at the focus located at $z = 0$ mm. A full-width-at-half-maximum (FWHM) value equal to 50 mm is measured for the 2P-OBIC axial profile. It is evident that as the sample is moved away from the focus or active region, the 2P-OBIC signal declines considerably. This behavior is a result of the spatial confinement of excitation in a two-photon process (Denk et al., 1990). Absorption of the energies of two-photons is restricted only at the focus resulting in the generation of free carriers merely on that small region. Electron-hole combination is not promoted in the other layers. Asymmetry in the axial profile is attributed to spherical aberration caused by the index of refraction mismatch introduced by the plastic packaging material (Xu & Denk, 1999; Kao et al., 1999; Ramsay & Reid, 2002).

A different situation is observed if the 1P-OBIC is considered. As shown in Fig. 3, 1P-OBIC is insensitive throughout the scanned axial positions. This is primarily due to the detection of the average photocurrents from all free carriers that are generated in the double-cone excitation along the optical axis. This results to 1P-OBIC having very poor axial resolution and can only convey information in two dimensions (2D). In contrast, the nonlinear generation of 2P-OBIC endows it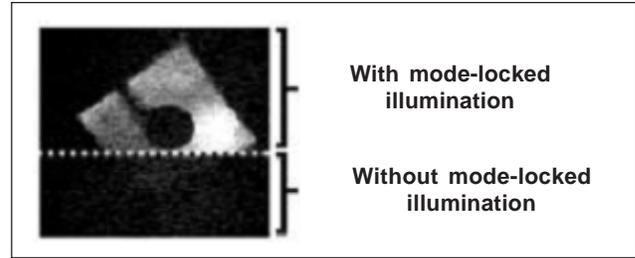 with an intrinsic optical sectioning capability enabling it to derive three-dimensional (3D) images even without confocal detection pinhole.

To illustrate further the sensitivity of 2P-OBIC signals, the LED sample is imaged at the focal position corresponding to the highest average photocurrent detected occurring at the active layer or $z = 0$ mm. Figure 4 shows the image of the LED affected by the presence of mode-locked illumination. During the period when the upper part of Fig. 4 is scanned, two-photon excitation occurs. The energy of two-photons is enough to induce a free carrier generation resulting in a detectable photocurrent.

Midway through the scanning procedure, the mode-locking mechanism of the femtosecond laser is turned off, converting the source to a continuous-wave laser. The quadratic requirement of two-photon generation can no longer be satisfied, resulting in the nondetection of the photocurrents at the observed sample positions. The energy of a single photon is therefore not enough to induce a photocurrent signal because it cannot transcend the LED band gap.

By comparing the images obtained using the 2P-OBIC and 1P-OBIC techniques, the advantage of two-photon excitation becomes more pronounced. Shown in Fig. 5 are the 2P-OBIC and 1P-OBIC images of the LED separated by 25 mm along the z axis. Average excitation powers at the sample were 1.5 and 0.06 mW for the two- and single-photon cases, respectively. The 2P-OBIC procedure exhibits superior image quality compared with 1P-OBIC. Since excitation is confined in the focal volume, free carriers are generated only at the focus. Absorption and scattering effects in 1P-OBIC images are eliminated (Xu & Denk, 1999). Two examples that will illustrate these effects are the
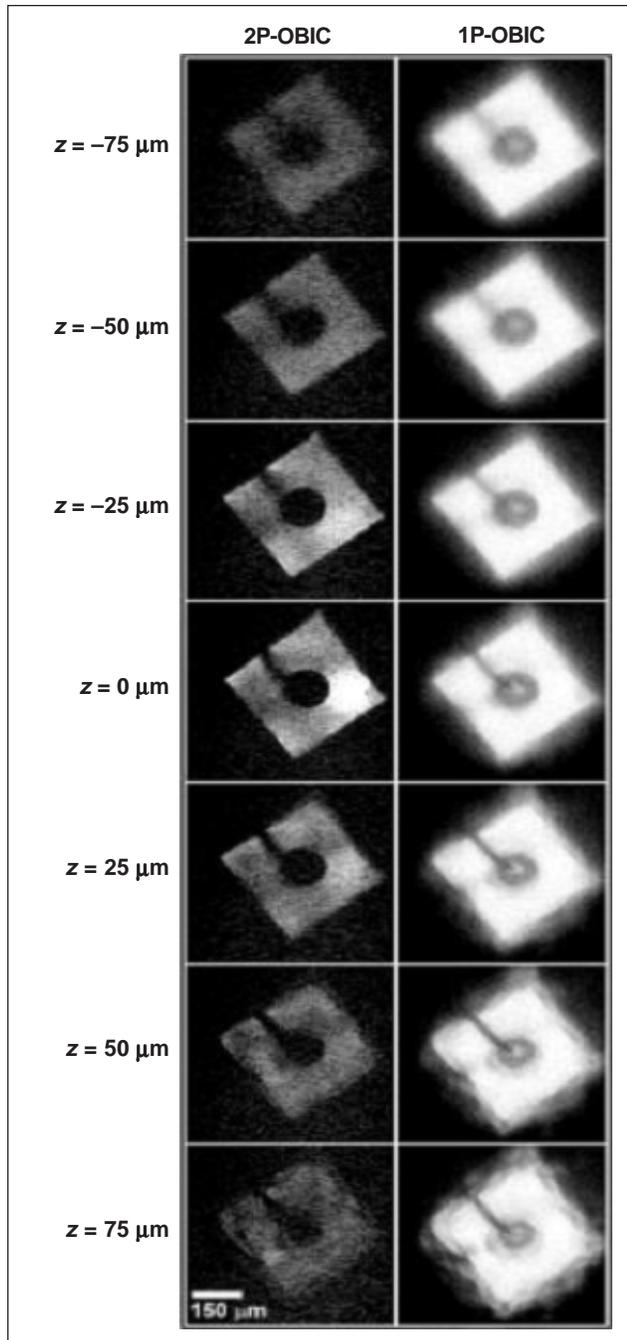
Fig. 5. Representative 2P-OBIC and 1P-OBIC images of the LED sample at different focal positions.

which becomes more prominent as the sample is moved towards the objective lens. These scattered photons are energetic enough to induce 1P-OBIC and introduce spurious signals to the image. The longer wavelength used for 2P-OBIC suffer less scattering and do not corrupt the image because they do not have enough power to satisfy the quadratic excitation power requirement.

The intrinsic optical sectioning capability of 2P-OBIC is clearly demonstrated in Fig. 5. It can be seen from the figures that the LED is optically sectioned by two-photon excitation attesting to the increase in axial resolution. On the contrary, 1P-OBIC images do not exhibit optical sectioning since the detected current is the average current across the whole excitation length. The most important effect of the nonlinear excitation of 2P-OBIC is the localized current topography on the LED surface. The nonuniformity of the OBIC generation points to the inhomogeneity of the absorption process which can be influenced by the 3D distribution of free carriers on the volume of the active region. This can be clearly mapped out by 2P-OBIC but cannot be seen by 1P-OBIC, giving us an insight to semiconductor properties that are inaccessible using 1P-OBIC.

CONCLUSION

In summary, optical beam-induced current imaging via two-photon excitation is demonstrated using light-emitting diodes. High-contrast images of LEDs exhibit a significant reduction of light scattering and absorption, thereby increasing the axial and spatial resolutions of the 2P-OBIC microscope. The nonlinearity of the excitation process enables it to image in 3D even in the absence of a confocal aperture. This revealed a localized absorption map of the semiconductor surface previously unseen by the 1P-OBIC technique.

ACKNOWLEDGMENT

differences in contrast of the electrodes and sharpness of the edges. In 2P-OBIC, the electrode appears dark and the edges appear sharp at all axial positions. However, in 1P-OBIC, a considerable amount of photocurrent is detected in the electrode regions and edges become enhanced due to wide-angle scattering,

REFERENCES

Cemine, V.J., B. Buenaobra, C.M. Blanca, & C. Saloma, 2004. High-contrast microscopy of semiconductor and metals sites in integrated circuits via optical feedback detection. *Opt. Lett.* **29:** 2479-2481.

Daria, V., J. Miranda, & C. Saloma, 2002. High-contrast semiconductor sites via one-photon optical beam-induced current imaging and confocal reflectance microscopy. *Appl. Opt.* **41**: 4157–4160.

Denk, W., J. Strickler, & W. Webb, 1990. Two-photon laser scanning fluorescence microscopy. *Science.* **248**: 73–75.

Kao, F., M. Huang, Y. Wang, M. Lee, & C. Sun, 1999. Two-photon optical beam-induced current imaging of indium gallium nitride blue light emitting diodes. *Opt. Lett.* **24**: 1407–1409.

Koyama, T., K. Sonoda, J. Komori, & Y. Mashiko, 1999. Detection of defects in metal interconnects by the nonbias optical-beam-induced current technique. *J. Appl. Phys.* **86**: 5949–5956.

Miranda, J. & C. Saloma, 2003. Four-dimensional microscopy of defects in integrated circuits. *Appl. Opt.* **42**: 6520–6524.

Ramsay, E. & D. Reid, 2002. Three-dimensional imaging of a silicon flip chip using the two-photon optical beam-induced current effect. *App. Phys. Lett*. **81**: 7–9.

Takasu, S., 2001. Application of OBIC/OBIRCH/OBHIC: Semiconductor failure analysis. *JEOL News*. 36E(1): 60-63.

Wilson, T. & C.J.R. Sheppard, 1984. Theory and practice of scanning optical microscopy. Academic Press Inc., New York.

Xu, C. & W. Denk, 1997. Two-photon optical beam-induced current imaging through the backside of integrated circuits. *Appl. Phys. Lett*. **71**: 2578–2580.

Xu, C. & W. Denk, 1999. Comparison of one- and two-photon optical beam-induced current imaging. *J. Appl. Phys.* **86**: 2226–2231.